University of Dayton
eCommons

Chemical and Materials Engineering Faculty Publications

Department of Chemical and Materials Engineering

2014

Less Is More: Long-Term in Vitro Exposure to Low Levels of Silver Nanoparticles Provides New Insights for Nanomaterial Evaluation

Kristen K. Comfort
University of Dayton, kcomfort1@udayton.edu

Laura K. Braydich-Stolle
Air Force Research Laboratory

Elizabeth I. Maurer
Air Force Research Laboratory

Saber M. Hussain
Air Force Research Laboratory

Follow this and additional works at: https://ecommons.udayton.edu/cme_fac_pub

Part of the Other Chemical Engineering Commons, Other Materials Science and Engineering Commons, Petroleum Engineering Commons, Polymer and Organic Materials Commons, and the Thermodynamics Commons

Less is More: Long Term *In Vitro* Exposure to Low-Levels of Silver Nanoparticles Provide New Insights for Nanomaterial Evaluation

Kristen K. Comfort[1,2] , Laura K. Braydich-Stolle[1], Elizabeth I. Maurer[1], Saber M. Hussain[1]*

[1]Molecular Bioeffects Branch, Air Force Research Laboratory, 2729 R St, Bldg 837, Wright-Patterson AFB, OH, 45433

[2]Department of Chemical and Materials Engineering, University of Dayton, 300 College Park, Dayton, OH 45469

AUTHOR EMAIL ADDRESS: saber.hussain@us.af.mil

RECEIVED DATE

CORRESPONDING AUTHOR FOOTNOTE: Saber M. Hussain, PhD, Tel: 937-904-9517, Fax: 937-904-9610

ABSTRACT

In view of the vast number of new nanomaterials (NMs) that require testing and the constraints associated with animal models, the majority of studies to elucidate nano-toxicological effects have occurred *in vitro*; with limited correlation and applicability to *in vivo* systems and realistic, occupational exposure scenarios. In this study, we developed and implemented a chronic *in vitro* model coupled with lower, regulatory dosages in order to provide a more realistic assessment of NM-dependent

consequences and illuminate the implications of long term NM exposure. When keratinocytes were exposed to 50 nm silver nanoparticles (Ag-NPs), we determined that chronically dosed cells operated under augmented stress and modified functionality in comparison to their acute counterparts. Specifically, Ag-NP exposure through a chronic mechanism increased p38 activation, actin disorganization, heightened ki67 expression, and extensive gene modification. Additionally, chronic Ag-NP exposure altered the way in which cells perceived and responded to epidermal growth factor stimulation, indicating a transformation of cell functionality. Most importantly, this study demonstrated that chronic exposure in the pg/mL range Ag-NPs did not induce a cytotoxic response, but instead activated sustained stress and signaling responses; suggesting that cells are able to cope with prolonged, low levels of Ag-NP exposure. In summary, we demonstrated that through implementation of a chronic dosimetry paradigm, which more closely resembles realistic NM exposure scenarios, it is possible to illuminate long-term cellular consequences which greatly differ from previously obtained acute assessments.

KEYWORDS: Chronic Exposure; Occupational dosage; Silver Nanoparticle; Stress Response; Gene Regulation; Risk Assessment

In light of their novel physicochemical properties nanomaterials (NMs) possess unlimited potential to advance current technologies in a diverse number of specialties. However, one considerable drawback is the unintentional cellular consequences that result following NM exposure, thus giving rise to the field of nanotoxicology.[1,2] Members of the scientific community have begun addressing the safety of NMs, evaluating their potential impact in terms of acute toxicity;[3,4] however their true influence in a physiological system has yet to be fully elucidated. This lack of current knowledge is due to a number of limitations, including poor NM characterization, incomplete study design, an inadequacy in the translation of *in vitro* results to an accurate *in vivo* prediction, and the inability to assess NM-induced bioeffects in a manner accurately representing a realistic exposure scenario.[5-7] Currently, the lion's share

of studies being performed employ an *in vitro* model due to time- and cost-restraints associated with animal models, as well as the sheer number of NMs that require testing.[8] These studies have identified a number of NM-induced bioeffects including augmented cellular stress, DNA damage, secretion of pro-inflammatory and immune markers, and cytotoxicity; indicating a high potential for long term health concerns associated with NM exposure.[9,10] However, there exists serious conflict with correlating acute, 24 hour *in vitro* NM exposure findings to a chronic *in vivo* model, illuminating the critical need for a new approach to feasibly and reliably assess NM consequences in cell culture.[11,12] One possible mechanism to increase NM-predictive modeling with *in vitro* systems is to extend exposure from acute to chronic durations. While minimal data exists regarding chronic NM introduction, one study successfully identified that after 24 weeks of exposure to carbon nanotubes, lung cells underwent a malignant transformation and developed a resistance to apoptosis.[13] This example clearly demonstrates why it is critical to examine long term NM bioeffects, as they were able to capture endpoints unobtainable through acute evaluation.

With regulatory guidelines already established on acceptable metallic exposure levels for bulk materials from agencies such as the Occupational Safety and Health Administration (OSHA) and the National Institute for Occupational Safety and Health (NIOSH), occupational limits have been set well below the high, dose-dependent concentrations typically examined in traditional nanotoxicology studies.[14] However, as nano-sized particles exhibit highly energetic and reactive properties significantly different from their bulk counterparts, the permissible exposure levels (PELs) of these metallic NMs will in all likelihood be even lower than the current bulk guidelines, once they are instituted. In fact, NIOSH has established guidance[15] on micron and nanosized titanium dioxide (TiO_2) materials that is considerably lower than the regulations for bulk TiO_2. Previously, the PEL for bulk TiO_2 exposure was listed at 15 mg/m^3 with a 5 mg/m^3 limit on the respirable fraction which accounted for the "fine" or micron sized exposures. After multiple *in vitro, in vivo,* and modeling studies were published the respirable limit has been lowered to distinguish between micron sized and nanosized TiO_2, with a PEL of 2.4 mg/m^3 and 0.3 mg/m^3 for micron- and nano-sized TiO_2, respectively. However, one of the

challenges associated with establishment of regulatory NM exposure guidelines is that the incomplete and conflicting reports of nanotoxicological responses make it impossible to set an exposure limit with confidence,[16] therefore, other frequently used NMs still do not have any revised regulations. Taken together, these issues further demonstrate the need for an enhanced means of examining NM bioeffects; including occupational exposure guidelines as a benchmark and developing a dosimetry paradigm that more accurately reflects real world exposure scenarios.

To address these aforementioned necessities, we designed and implemented a chronic, *in vitro* exposure model for the improved safety assessment of NMs at low, realistic dosages. Keratinocytes, the HaCaT cell line, underwent daily exposure for 14 weeks to 50 nm silver nanoparticles (Ag-NPs) at levels based on the permissible OSHA limits for bulk silver. Ag-NPs were chosen as a proof of concept for this study as their bioresponses have been extensively studied and are well established, providing a baseline for experimental design.[17-21] The stress response of these chronically dosed cells was evaluated and directly compared against a 24 hour acute exposure at a concentration equal to the cumulative Ag-NP dosage the chronically exposed cells encountered over the 14 week study (Figure 1). Our analysis revealed that chronically dosed HaCaTs functioned under augmented cellular stress and altered functionality, as evaluated through several key endpoints focused on stress markers, gene regulation, and cellular response to epidermal growth factor (EGF) stimulation. We believe that this study demonstrated the capability of a chronic dosimetry paradigm to provide enhanced *in vitro* assessments and to elucidate sustained cellular responses to NM exposure.

RESULTS AND DISCUSSION:

Chronic exposure model: System design requirements and procedures. The critical design elements incorporated into this chronic *in vitro* model included; 1) a mechanism for daily delivery of a precise, low NM dosage, 2) the ability for an extended experimental time frame, and 3) the incorporation of a characterized, robust non-cancerous cell line. As dermal contact is a primary source of NM exposure[22] the keratinocyte cell line, HaCaT, was selected for this proof of concept study, owing

to its establishment as a model for nanotoxicology investigation and its well-documented cellular processes.[23,24] Furthermore, HaCaTs have been repeatedly used for investigations into intracellular fate and behavior of NMs;[25,26] resulting in a sound understanding of how these cells respond following NM challenge. Additionally, the use of HaCaTs is further validated by the fact that this immortalized cell line was isolated from the basal layer of the epidermis, which has been shown to be a principle location of particle accumulation, independent of mode of NM entry.[27]

For chronic exposure, the HaCaTs were sub-cultured weekly in 6-wells plates and dosed with predetermined concentrations of NMs for 8 hours a day, 5 days a week, for a duration of 14 weeks (Figure 1). This model was designed to mimic an occupational exposure scenario as closely as possible under the constraints of an *in vitro* setting. After the 8 hour exposure, the NM-contained media was removed and stored for later examination, while the cells were washed and replenished with fresh media. The HaCaTs were split weekly to an optimized density of viable cells, followed by their initial growth for 64 hours free of NMs; representative of a worker's removal from NM contact over the weekend. Negative controls, which incurred no NM introduction, were included in the chronic experimental design to identify any cellular modifications due to an aging effect.
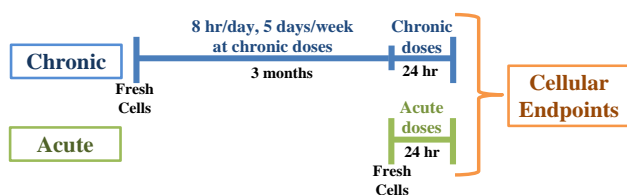
Figure 1. Timeline for chronic and acute Ag-NP exposure. At the onset of experimentation, identical vials of fresh HaCaTs were prepared and stored. Chronically exposed cells underwent NM exposure 8 hours per day, 5 days a week for 14 weeks. After that duration, fresh cells were prepared for acute trials and all HaCaTs underwent a 24 hour NM exposure to allow for direct and simultaneous comparison of acute and chronic dosimetry conditions. Cellular endpoints that targeted the stress and EGF signaling response were then evaluated.

Silver nanoparticle selection and dosimetry. For the initial test of the designed chronic exposure system, silver nanoparticles (Ag-NPs) were viewed as advantageous for multiple reasons, and thus selected as the choice NM. Firstly, cellular behavior following Ag-NP introduction has been extensively studied with robust cytotoxic and stress responses well-documented.[18-20] Furthermore, due to their antimicrobial and plasmonic properties, Ag-NPs incur the highest incorporation in consumer and medical products to date.[28] As the majority of these products have direct contact with the skin, including clothing, cosmetics, bandages, and personal electronics, the selection of silver as a proof of concept for the chronic HaCaT model was especially appropriate. Additionally, OSHA and NIOSH regulatory guidelines exist for silver, in bulk form, providing an initial dosage set-point for testing Ag-NP concentrations at more realistic, occupational exposure values (Table 1). Established safety limits for bulk silver are provided for soluble form, insoluble form, and levels that are "immediately dangerous to life and health" (IDLH).

Table 1. Chronic Dosages were Calculated from Established Occupational Exposure Levels

OSHA Safety Limits for Silver		Chronic Dosage (4% of OSHA Limit)	Acute Dosage (Chronic dose x 70 days)
Soluble Level	10 pg/mL	0.4 pg/mL	28 pg/mL
Insoluble Level	100 pg/mL	4 pg/mL	280 pg/mL
IDLH	10 ng/mL	400 pg/mL	28 ng/mL

Owing to the vast differences in physical properties when a bulk material is reduced down to the nanoscale and lack of regulatory guidelines for NM exposure, selection of meaningful dosages for nanotoxicity examinations has always been a major challenge. For this study, daily exposure concentrations of Ag-NPs were based off the OSHA regulatory values for bulk silver and incorporated an adjustment to account for the fact that 2-4% of all introduced Ag-NPs, independent of mode of exposure, are retained in the skin (Table 1).[29] As no regulatory values for Ag-NPs are currently in place, these chronic dosages, spanning 0.4 to 400 pg/mL, which combined bulk occupational limits and known retention rates, provide a plausible NM daily exposure range. The acute exposure Ag-NP concentrations

were equivalent to the cumulative mass of Ag-NPs encountered over the 14 week duration (70 days of exposure), thus removing the variable of total mass from this experiment. As seen from Table 1, both the chronic and acute dosages are well below the traditional dose-dependent concentrations previously examined, which are typically in the µg/mL range.

Nanoparticle characterization. To verify particle quality and assess target parameters, extensive characterization of the 50 nm Ag-NPs was performed prior to cellular introduction (Table 2).[30,31] TEM imaging confirmed the primary particle size of approximately 50 nm and spherical morphology (Figure 2A). The degree of Ag-NP agglomeration and zeta potential were ascertained in growth media, as that is the primary working environment in this study. A slight increase in effective particle diameter was determined, and is in agreement with the minimal aggregation brought on by the creation of a protein corona.[32] Furthermore, there was little variation in agglomerate size indicating a uniformly monodispersed set of Ag-NPs. The zeta potential analysis identified a particle surface charge of -10 mV, which is brought about by the formation of a protein corona with negatively charged serum proteins.[33] To verify the known cytotoxic response of this Ag-NP stock, a traditional dose dependent viability assessment was performed to determine the LD_{50} value, which was found to be 54.3 µg/mL (Table 2, Supporting Information Figure 1A).

Table 2. Silver Nanoparticle Characterization

Assessment	Start of Study - Media	End of Study - Media	Lysosomal Fluid
Primary size (nm)	54.3 ± 5.3	52.5 ± 5.1	--
Agglomerate size (nm)	101.9 ± 3.3	142.1 ± 10.8	336.8 ± 17.5
Zeta potential (mV)	-9.90 ± 0.4	-9.2 ± 0.2	-5.9 ± 0.4
Ionic dissolution (%)	0.32 ± 0.04	0.62 ± 0.01	8.89 ± 0.07
Deposition efficiency (%)	52.8 ± 4.8	59.9 ± 7.0	--
LD_{50} (µg/mL)	54.3	47.7	--

It has been identified that the physicochemical properties of NMs can alter over time, thus modifying the nature of both the nano-cellular interface and the induced bio-responses.[34] Therefore, Ag-NP characterization was also performed at the end of the three month study to ascertain if any time-

dependent modifications existed (Figure 2B and Table 2). From the TEM image, a small degree of particle fusing was identified with the older Ag-NP samples. This modification was also reflected in the DLS data in which a minimal increase in particle agglomeration existed after the 14 week duration; although still not to a large extent. A slight drop in the LD_{50} value was found, which is in agreement with published reports that indicated a time dependent increase in the toxic potential of Ag-NPs.[35] On the whole, however, minimal modifications to the Ag-NPs were seen throughout the duration of this study, indicating the particle quality and behavior were retained.
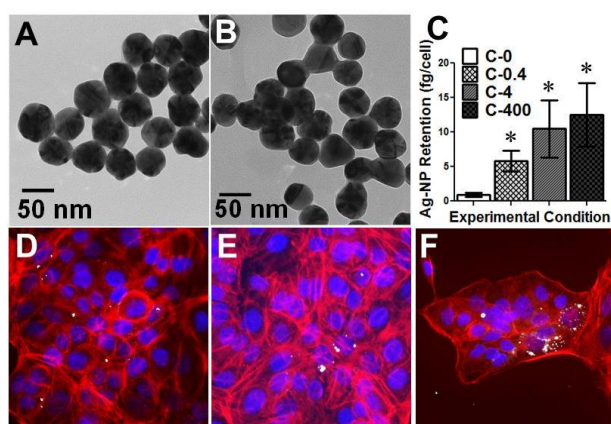
Figure 2. Time Dependent Characterization and Internalization of Ag-NPs. Representative TEM images of 50 nm Ag-NPs (A) at the beginning of chronic exposure and (B) at the end of the 14 week study. (C) After 14 weeks of exposure to low dosages of Ag-NPs the degree of Ag-NP internalization was ascertained. Fluorescent images captured the internalized Ag-NPs at the end of the chronic dosimetry following daily exposure to (D) 0.4 pg/mL, (E) 4 pg/mL, and (F) 400 pg/mL. HaCaT cells underwent actin (red) and nuclear (blue) staining with metallic NPs reflecting white.

As the dissociation of Ag-NPs into elemental ions has been identified as a root cause of nanotoxicity,[36] the percent dissociation of the Ag-NPS after 8 hours in media was evaluated to determine if this phenomenon would be a major factor. At the start of the study, the generation of silver ions was found to be minimal, only a 0.32% dissolution rate (Table 2). As NP age has been shown to

8

dictate the kinetic rate of dissolution, [35] this analysis was repeated after 14 weeks. At the end of the study, the 50 nm Ag-NPs did display a higher degree of silver ion generation, however, this final rate was still a minor factor, only 0.58%.

The deposition efficiency at the 400 pg/mL chronic dosage was evaluated to determine the extent of Ag-NP/HaCaT association. After 8 hours incubation, it was quantitatively determined that approximately 55% of the Ag-NPs were either internalized or strongly associated with the cellular environment (Table 2). It was also found that Ag-NP age had a negligible influence on this aspect of particle behavior. Following binding to the cell surface, NPs are typically internalized through a combination of endocytosis mechanisms, temporarily stored in intracellular vesicles, and marked for either degradation or exocytosis. [37,38] Owing to the facts that NPs are internalized into lysosomes and that NMs display significantly altered behavior in physiologically relevant environments, [34,39] the Ag-NPs were re-characterized in artificial lysosomal fluid (ALF). Following an 8 hour incubation in ALF at 37 °C, evaluation of the agglomerate size, zeta potential, and ionic dissolution of the Ag-NPs were carried out with a substantial increase identified for NP agglomeration and dissolution rate (Table 2). Due to previous reports and the low pH of ALF, [40] these results were not surprising, however, they are significant as they demonstrate the potential for increased ion production following internalization.

Another dosimetry concern is that due to the continual proliferation of cells and the fact that the rate of NP internalization is a function of cell cycle state, [41] cells within a culture are not necessarily exposed to equal NP quantities. However, the daily exposure incorporated into the design of this study should minimize this variability, as HaCaT cells were continually exposed to Ag-NPs throughout their cell cycle progression; normalizing the quantity each cell was exposed to over its life cycle.

In light of the importance of dosimetry and uptake, the ability of HaCaTs to internalize Ag-NPs over an extended time frame was assessed quantitatively and qualitatively through ICP-MS and CytoViva imaging, respectively (Figures 2C-2F). We identified small amounts of intracellular Ag-NPs from both analyses after 14 weeks of daily exposure, further validating the observed degree of Ag-NP deposition and slow dissolution rate at the tested low dosages.

Long Term Ag-NP Exposure Resulted in Augmented and Sustained Stress Responses. Firstly, after 14 weeks exposure, the HaCaTs exhibited a minimal change in the number of viable cells (Supporting Figure 1B); with a slight diminishment in cell number (less than 10%) associated with the 400 pg/mL condition. This response is believed to be due to a decreased cell growth rate as a result of elevated stress levels, and not necessarily the induction of apoptosis.[42] It is also imperative to highlight the fact that at levels in the pg/mL region, the HaCaTs were able to handle sustained Ag-NP exposure without the subsequent cytotoxic response, typically associated with nanosilver. Next, a primary set of endpoints were developed around the evaluation of recognized stress markers, and included target protein activation, actin coverage, cytokine secretion, and modifications to gene regulation. To interpret the role of daily 50 nm Ag-NP exposure, chronically exposed HaCaTs were directly compared to cells that underwent a 24 hour, acute exposure to a dose equivalent to the cumulative Ag-NPs encountered by the chronic cells (Figure 1 and Table 1). Results from these analyses demonstrated a distinct, differential response between chronically dosed HaCaTs at the 400 pg/mL concentration and their acute counterpart (28 ng/mL); with chronic exposure resulting in an amplified, sustained stress reaction (Figure 3). Furthermore, the cellular responses to Ag-NP concentration at the 0.4 and 4 pg/mL dosages produced very similar result patterns to the 400 pg/mL data sets; which we believe to be due to the fact that at these extremely low dosages, cells are not able to accurately sense the difference in Ag-NP concentration. Therefore, for conciseness, the 0.4 and 4 pg/mL results are presented in Supporting Information Figures 2 and 3.

The p38 mitogen-activated protein kinase family members have been shown to be activated by a variety of extracellular stress stimuli and initiate a hierarchy of protein and transcription regulators of apoptosis, immune response, migration, and gene regulation.[43] Chronic stimulation with low levels of Ag-NPs resulted in an increase of the phosphorylation and activation of p38 over control and acutely dosed samples (Figure. 3A). While acute exposure to Ag-NPs has been previously shown to increase p38 activation in other biological models,[44,45] at the low dosages selected for this study no such increase

was detected. One downstream response of stress-induced p38 is the reorganization and increased expression of actin filaments.[46] With increased degrees of cellular stress the actin loses its normal structure and becomes disorganized; as shown following chronic exposure (Figure 3B). While both acutely and chronically exposed cells indicated a larger percentage of actin coverage over controls, the chronic cells displayed a higher degree of disruption; as easily identified by the globular nature of the actin in the representative confocal images.
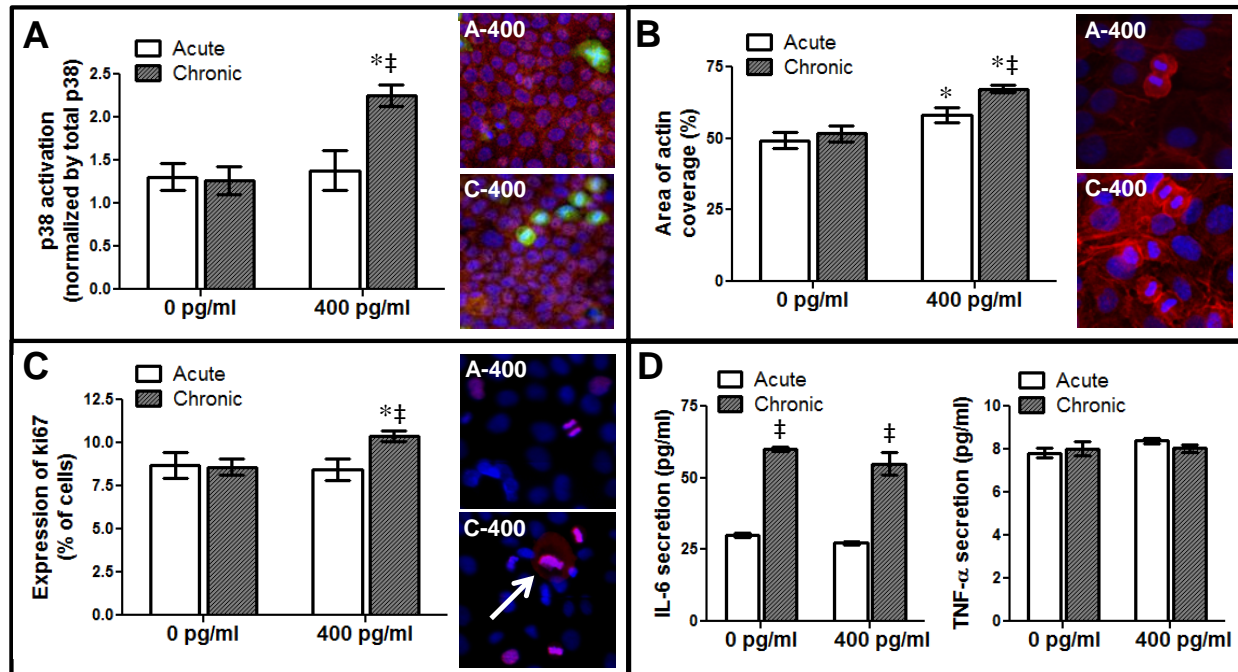
Figure 3. Ag-NP Induced Stress Response is Dependent on the Means of Exposure. Evaluation of known cellular stress responses was carried out following introduction of 50 nm Ag-NPs through either an acute (A-400) or chronic (C-400) exposure scenario. (A) Confocal imaging evaluation of p38 signal transduction activation was performed through detection of the phosphorylation state (green) and normalized by total p38 (red). Included are representative confocal images of acute and chronically dosed cells. (B) Degree of actin (red) coverage over the cellular area was determined and representative images included under acute and chronic conditions for Ag-NP introduction. (C) The number of cells that were actively expressing ki67 (pink) and its cellular localization were evaluated in acutely and chronically dosed HaCaT cells. (D) The quantities of secreted pro-inflammatory cytokines IL-6 and TNF-α were ascertained through ELISA experimentation. Recall, equivalent acute dosage for the 400

pg/mL condition was 28 ng/mL. For all figure sections, a two way ANOVA with Bonferroni post-test was run with * denoting significance from untreated and ‡ denoting significance from the acute at the same concentration. (n=3, p<0.05)

In addition to its recognized role in cell proliferation, ki67 also has a critical secondary function in the repair of damaged DNA.[47] As Ag-NP cellular exposure has been strongly correlated to DNA damage,[48] the activation and location of ki67 was of great interest to this study. Our results demonstrated an enhanced ki67 expression in chronically dosed cells as well as both nuclear and cytosolic localization, with no significant alterations noted in the acute cells (Figure 3C). We hypothesize that this augmented expression is due to the continual synthesis of ki67 over the course of this experiment, in an attempt to repair the persistent DNA damaged caused by Ag-NP presence. The cytosolic identification is indicative of excess ki67 cellular production and its directed shuttling out of the nucleus for targeted degradation, supporting the supposition of its role in DNA damage.

Beyond stress markers Ag-NPs have been linked to the induction of the inflammatory response, which if found to be sustained could introduce serious health implications.[49] One early stage action of the inflammatory response is the cellular secretion of pro-inflammatory cytokines, including IL-6 and TNF-α. For both the Ag-NP treated and un-treated chronic conditions, a significant amount of IL-6 was produced from the HaCaT cultures (Figure 3D), indicating that this phenomenon could be an aging effect of the chronic growth conditions, and not specific to Ag-NP stimulation. To verify this, a time course analysis was performed (Supporting Information Figure 3B) that demonstrated sustained secretion kinetics, brought on by the daily removal and washing processes which continually disrupted the cellular accumulation and equilibrium of IL-6. The concentration of secreted TNF-α was also evaluated with negligible quantities detected for all experimental conditions (Figure 3D). Taken together, these data sets indicate that the low chronic Ag-NP concentrations did not substantially active pro-inflammatory responses.

12

As chronically dosed HaCaTs displayed augmented cellular stress responses compared against acute exposure, we hypothesized that genetic modifications were also present in stress dependent genes. The legitimacy of this supposition was evaluated using a stress and toxicity focused, real time PCR array. This PCR array profiled the expression of 84 genes that have been previously identified as key regulators of cellular stress and apoptosis responses. The array analysis identified that both acutely dosed and chronically undosed cells displayed modified gene regulation for 3 of the 84 examined genes (Table 3). Following acute Ag-NP exposure, as expected, there was an increase in heat shock protein (HSP) and DNA repair genes. HaCaT aging controls showed an upregulation of IL-6, in agreement with previous data. However, while these conditions demonstrated only slight modifications to stress and toxicity based gene regulation, HaCaT cells chronically dosed with regulatory-based Ag-NP concentrations displayed a considerable alteration to their genetic profile with 12 of the 84 genes undergoing a significant variation (Table 3).

Table 3. Enhanced Stress-Based Gene Modulation Following Chronic Exposure

		Fold Change over control cells[a]		
Stress Response Genes		**Acute – 28 ng/mL**	**Chronic – 0 pg/mL**	**Chronic – 400 pg/mL**
Gene	Function			
CCL21	Immunoregulation & inflammatory response	-	-	-3.37
CCND1	Cell cycle progression	-	-	2.94
CYP1A1	Metabolism and lipid synthesis	-	2.56	3.31
CYP7A1	Metabolism and lipid synthesis	-	-	-3.15
EGR1	Differentiation and mitogenesis	-	-	2.45
GDF15	Differentiation and maintenance	-	-	2.23
GSTM3	Stress response	-	-	2.40
HSPA1L	Stress response	3.62	-	-
HSPA8	Stress response	2.05	-	2.50
IL6	Inflammatory response	-	5.72	6.09
PTGS1	Inflammatory response	-	-2.61	-3.69
RAD23A	DNA damage	3.71	-	3.60
SERPINE1	Fibrinolysis inhibitor	-	-	6.12

[a] Reported genes displayed a ≥ 2.0 fold regulation over the control (acute undosed condition) and statistical significance. Data represents three independent trials with $p < 0.05$. "-" indicates that no statistically significant change was observed.

From this analysis it was identified that the primary genes altered following chronic Ag-NP exposure fall into the classes of inflammatory response, stress response, and cell regulation. While the stress and inflammatory activators were expected from previous results, the marked alteration to genes involved in cellular regulation indicated that sustained disruption to cellular homeostasis occurred; as fundamental cellular behavior is dictated by gene regulation. Furthermore, the identified genes regulated in the chronic undosed controls were all equally modified in the chronically dosed conditions, validating the supposition that they are aging related effects. Taken together, this study identified that chronic exposure to Ag-NPs induced a considerable alteration to the basal gene regulation involved in the stress response, with previously unexplored biological consequences.

Altered EGF Signal Transduction Efficiency. From these results, it is clear that HaCaT cells undergoing chronic exposure to 50 nm Ag-NPs developed high basal stress levels and displayed substantial genetic modification. Therefore it appeared highly probable that the functionality of these cells also became modified over the duration of this study. The primary function of keratinocytes is to recognize and respond to EGF stimulation, resulting in a proliferative, migratory, or anti-apoptotic cell outcome. Based on the known importance of EGF signal transduction in keratinocyte behavior, the fact that EGF signaling has been previously altered by the presence of Ag-NPs,[20] and that excessive cellular stress has been linked to a modification of EGF receptor (EGFR) expression,[50] EGF signaling efficiency was selected as the best metric to evaluate HaCaT functionality. Following EGFR activation, one of the first dependent signaling events is the induction of the PI3K/Akt and the Ras/Erk pathways. Evaluation of the phosphorylation states of both Akt and Erk revealed a higher degree of activation of these key signaling proteins in the chronically dosed experimental conditions (Figure 4 and Supporting Information Figure 4). Interestingly, at these reduced Ag-NP levels, the acutely dosed samples demonstrated no alterations compared to control cells, indicating that this response was progressively built up over time.

Going further into the EGF-dependent signaling response, a PCR array analysis, focused on EGF signal transduction genes, was performed to identify any alterations to the EGF signaling network on the genetic level (Table 4). The genes profiled in this real time PCR array have all been strongly linked to signaling dependent activation following EGF stimulation. Analogous to the previous stress-based gene array results, acutely dosed and chronic undosed displayed minimal alterations, with only 1 gene modified of the 84 examined. On the contrary, chronic introduction of Ag-NPs induced high modifications to the HaCaT genetic response following EGF stimulation. The classes of genes targeted by chronic exposure are primarily signaling and matrix/migration genes. Of particular interest is the overexpression of Akt, MAPK, PRKCA, STAT3, and STAT5A, which are major signal transduction mediators and are in agreement with the observed increased EGF-dependent signaling. Additionally, chronically dosed cells displayed an over 9 fold up-regulation of MMP7, which is downstream of p38 and responsible for breaking down extracellular matrix.[51] When taking the previously identified increase in expression and disorganization of actin filaments under consideration, it suggests that the overexpression of MMP7 could be a cellular defense mechanism to counteract this response.
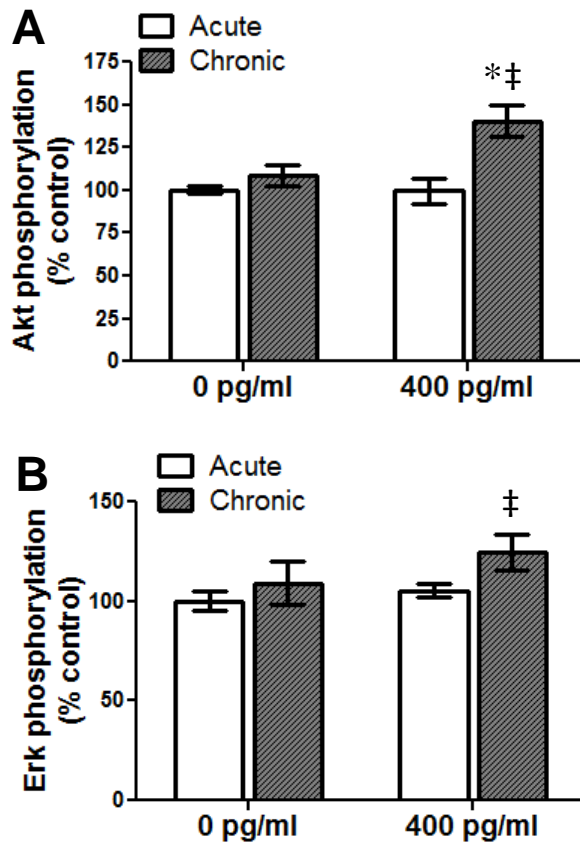
Figure 4. Modification to EGF-Dependent Akt and Erk Activation. The ability of Ag-NPs to influence the efficiency of EGF-dependent signal transduction was evaluated through the extent of (A) Akt phosphorylation and (B) Erk phosphorylation following stimulation with 10 ng/mL EGF. Recall, equivalent acute dosage for the 400 pg/mL condition was 28 ng/mL. A two way ANOVA with Bonferroni post-test was run with * denoting significance from untreated and ‡ denoting significance from the acute at the same concentration. (n=3, $p<0.05$)

The EGF receptor contains two primary tyrosine sites for phosphorylation (Y1068 and Y1173). The tyrosine site that is selectively phosphorylated dictates the mechanism through which the cells respond to EGF. Moreover, the balance between Y1068 and Y1173 selection has been previously shown to be susceptible to oxidative stress.[52] As the HaCaT response to EGF stimuli was seen to be significantly different for acutely versus chronically dosed cells, it logically follows that this tyrosine selection was also modified. For chronically dosed cells, Y1068 was preferentially phosphorylated, while the acutely

dosed cells enhanced Y1173 phosphorylation (Supporting Information Figure 4). This transformed means of EGF receptor activation coupled with the genetic modifications, we believe, resulted in the ability of the chronically dosed cells to display a modified innate response to EGF stimulation, as proven through enhanced signaling efficiencies.

Table 4. Alteration to EGF-Dependent Gene Regulation by Chronic Ag-NP Exposure

		Fold Change over control cells[a]		
EGF Dependent Genes		**Acute – 28 ng/mL**	**Chronic – 0 pg/mL**	**Chronic – 400 pg/mL**
Gene	Function			
AKT1	Cell cycle progression, signaling, and survival	-2.57	-	-
AKT3	Cell cycle progression, signaling, and survival	-	-	4.27
BCAR1	Cell migration	-	-	2.22
CCND1	Cell cycle progression	-	-	2.90
FN1	Cell adhesion and migration	-	9.86	5.06
MAP2K7	MAPK protein involved in stress signaling	-	-	2.04
MMP7	Breakdown of extracellular matrix	-	-	9.40
PRKCA	Signaling protein with multiple roles	-	-	3.94
STAT3	Mediates cellular response to growth factors	-	-	2.08
STAT5A	Mediates cellular response to growth factors	-	-	2.13

[a] Reported genes displayed a ≥ 2.0 fold regulation over the control (acute undosed condition) and statistical significance. Data represents three independent trials with $p < 0.05$. "-" indicates that no statistically significant change was observed.

Chronic Ag-Np Exposure Generates an Augmented Stress Response. The fact that Ag-NPs introduced a cellular stress response is not a new concept to toxicologists;[18,20,21] however the sustained bioeffects observed as a result of sustained exposure is a growing concern that needs to be further explored. The results presented here indicated that even at exceptionally low concentrations of Ag-NPs, chronically dosed HaCaT cells displayed an augmented, sustained cellular stress response. The numerous endpoints and multiple Ag-NP concentrations tested further support this conclusion. Furthermore, Ag-NPs are notoriously recognized for their ability to induce a strong cytototoxic

response,[17,19] however, in this study chronic introduction of regulatory dosages were associated with negligible loss of cell viability.

The Ag-NP dependent induction of stress markers has previously been shown to be dose dependent,[19] which makes these results even more intriguing. As chronically dosed cells displayed a higher stress response versus the acutely dosed, this indicates that the degree of stress activation is not only a function of particle concentration, but also of exposure duration. This supposition was further verified by examination of the HaCaT stress and signaling responses following a 5 µg/mL acute exposure (Supporting Information Figure 5). For all experimental endpoints, the extremely higher 5 µg/mL dose correlated with a lower induction of stress than was seen with the 400 pg/mL chronic condition. This analysis suggests that no matter what dosage is used, chronic NM exposure results in biological responses unobtainable from acute methodologies. As such, it appears probable that the HaCaT cells not only built up these cellular responses over time, but that their genetic makeup was altered in such a way that allowed for adaptation to continual stress. In agreement with the stress results, acute exposure to 5 µg/mL Ag-NPs produced a differential EGF signaling response with an approximate 20% drop in Akt and Erk phosphorylation. This comparison between acute and chronic EGF signaling supports the aforementioned supposition of modified functionality, as how keratinocytes respond to EGF is a critical part of their innate behavior.

Extended Retention and Ionic Dissolution of Ag-NPs. As earlier discussed, Ag-NPs are being rapidly included in a score of consumer products, including medicines, clothing, toothpaste, cosmetics, food storage containers, home appliances, and bandages.[28] When taken together it appears that consumers are experiencing nearly continuous exposure to engineered NMs; necessitating the performance of long-term exposure studies. Moreover, it has become apparent that the cytotoxic and antimicrobial potential of Ag-NPs is due to the ionic dissolution and the generation of silver ions.[34,36] In fact, a recent study found that silver was released from antibacterial fabrics in an artificial sweat solution,[53] demonstrating the potential of silver particles and ions to be transported from that material to

skin in low dosages over an extended duration. This fact, coupled with our findings that cells are able to retain Ag-NPs following exposure at extremely low dosages, introduces the question of whether the observed chronic effects were brought on by the Ag-NPs themselves, the generated silver ions, or a combination of both.

To answer this question, HaCaTs were chronically exposed to silver nitrate at the equivalent Ag-NP concentration (400 pg/mL) or a concentration equal to the determined dissolution rate after 8 hours in media (1.28 pg/mL). After a duration of 14 weeks, these silver-ion exposed cells underwent the same stress and EGF signaling endpoint analyses as performed on the Ag-NP exposed HaCaTs (Figure 5). It was found that exposure to 1.28 pg/mL silver nitrate had a negligible impact on HaCaT cultures (Figure 5A). While the 400 pg/mL silver nitrate did cause stress responses, it was not comparable to the quantities associated with chronic Ag-NP introduction. Furthermore, Akt and Erk phosphorylation states remained unchanged following chronic exposure to low levels of silver nitrate (Figure 5B), in direct contradiction to Ag-NP treated cultures. Lastly, these dosages of silver nitrate did not impact cell viability over the course of this experiment (Supporting Information Figure 6). Taken together, these results suggest that the observed, sustained bioresponses to Ag-NPs are a combination of both the disruptive presence of the particles themselves and the production of silver ions through dissolution. We believe that this joint NP and ion explanation is founded in the fact that Ag-NPs are retained within cells over time, which compounds the production of ions and initiation of stress, owing to the fact that increased dissolution was associated with a lysosomal environment. While this does not completely elucidate the mechanisms behind the observed stress and signaling responses to chronic Ag-NP exposure, it does provide valuable insight in how the continued exposure and particle retention may be induces cellular modifications.
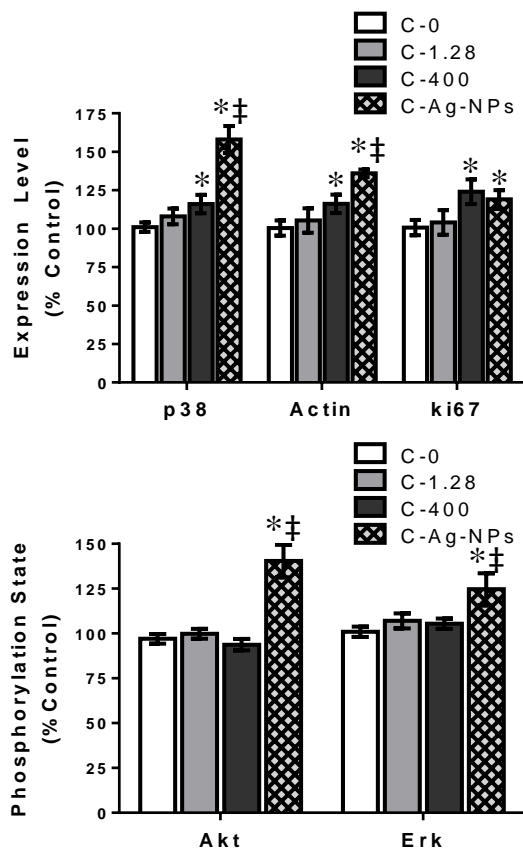
Figure 5. Bioeffects of chronic exposure to silver ions. Following sustained exposure to silver nitrate at dosages of 1.28 pg/mL (C-1.28) and 400 pg/mL (C-400) the stress and signaling responses were evaluated and compared against the chronic 400 pg/mL Ag-NP data (C-Ag-NPs). (A) Expression levels of p38, actin, and ki67 were determined through immunofluorescence and compared against an acute untreated control. (B) Normalized phosphorylation levels were assessed following exposure a 2 hour exposure to 10 ng/mL EGF. For all data sets, a two way ANOVA with Bonferroni post-test was run with * denoting significance from the untreated acute control and ‡ denoting significance between 400 pg/mL silver nitrate and Ag-NP conditions. (n=3, p<0.05)

Can this New NM Exposure Paradigm Aid in Establishment of Regulatory Limits? This study presents a new means through which the cellular responses of NMs are evaluated; implementing a chronic *in vitro* model in conjunction with low NM dosages. This system was designed to mimic an occupational exposure, in which NMs are introduced 8 hours a day and 5 days per week at levels based

20

on OSHA guidelines. Herein lies a major concern; that there is limited to no regulatory and occupational exposure limits in place for NMs, due to the conflicting reports of their dependent cellular responses[14] and lack of correlation between *in vitro* and *in vivo* systems.[12]

One long term goal of this work is to evaluate whether this chronic *in vitro* model can be extrapolated to improve *in vivo* response predictions. As extended NM exposure allows for the cells to modify their behavior and establish a new basal homeostasis, we believe it offers a plausible mechanism to bridge the gap between *in vitro* and *in vivo* models, improve correlation efficiencies, and aid in the establishment of NM regulatory guidelines. Included within these future plans are to expand cell models beyond HaCaTs to include additional, key organs targeted by NMs, such as neuronal, liver, and kidney cell lines.[54,55] Through the combination of coupling specific NMs to their known cellular targets and the application of the chronic exposure model, we believe this will provide a conceivable means for a finely honed analysis of predictive toxicological responses that accurately aligns with previous *in vivo* data.

CONCLUSIONS:

In this study, an *in vitro* model was successfully designed and implemented to provide a mechanism to assess implications of NMs at realistic exposure levels over an extended period of time. This distinct approach allowed for the utilization of low, regulatory doses applied over 14 weeks, which more closely mimics an *in vivo* exposure scenario, but retains the advantages associated with an *in vitro* assessment. Through proof of concept experimentation that utilized 50 nm Ag-NPs and keratinocyte cells, this study identified that in the absence of significant cytotoxicity, distinctive cellular responses arose between the chronically and the acutely dosed cells; including a long term stress response, substantial modifications to gene regulation, and an increased EGF signaling efficiency (Figure 6). Using silver nitrate as a control, it was ascertained that these responses were brought on by a combination of the particles themselves and their ionic dissolution. These results demonstrate the effectiveness of a chronic *in vitro* model to elucidate the long term implications of NM exposure that were previously unobtainable; improving the ability to accurately evaluate the safety of engineered NMs.
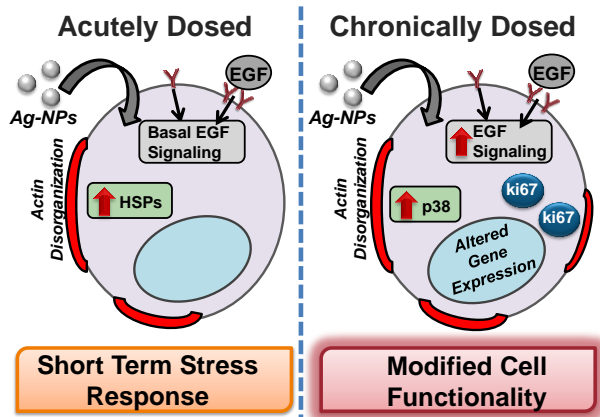
Figure 6. Summary of the differential response to Ag-NPs following execution of a chronic dosimetry delivery system. HaCaTs that underwent a one-time, 24 h exposure to Ag-NPs displayed minimal cellular alterations. On the contrary, cells that were exposed to the same amounts of Ag-NPs, but through a through a chronic exposure means, demonstrated significant cellular consequences, including sustained stress levels, alterations to EGF response, and modified gene expression.

METHODS:

Silver nanoparticle characterization. Citrate stabilized Ag-NPs with a primary particle size of 50 nm were purchased from nanoComposix in solution form. Verification of primary size and spherical morphology was carried out through TEM analysis (Hitachi H-7600) at 120,000x magnification. The effective particle size and surface charge were determined with dynamic light scattering and zeta potential procedures, respectively, using a Malvern Zetasizer Nano-ZS.[56] The degree of particle dissolution after 8 hours at 37 °C was evaluated by separation of released ions from the Ag-NPs through tangential flow filtration (Kros Flo Research System, Spectrum Labs) and silver content analysis on a Perkin Elmer NexION 300D inductive coupled plasma mass spectrometry (ICP-MS). ALF was constructed from a previously published recipe[57] and used to evaluate the dissolution rate in intracellular vacuoles. The deposition efficiency was determined by the incubation of HaCaT cells with 400 pg/mL Ag-NPs for 8 hours at 37 °C, the chronic exposure conditions; followed by the removal and quantification of silver within the supernatant *via* ICP-MS analysis.

Implementation of a chronic *in vitro* model for nanoparticle exposure. The human keratinocyte cell line HaCaT were a kind gift from the Army Research Laboratory and cultured in RMPI-1640 medium (ATCC) supplemented with 10% heat inactivated fetal bovine serum (ATCC) and 100 U/mL penicillin and 100 µg/mL streptomycin. To mimic occupational exposure, cells were exposed to the stated Ag-NP concentrations (2 mL) for 8 hours per day, Monday through Friday. After the 8 hour exposure, the media was collected and stored at -80 ºC, and cells were washed and replenished with fresh media. HaCaT cultures were split every Friday evening to a density of 5 X 10^4 viable cells per well in a 6-well plate and incubated at 37ºC in a humidified atmosphere containing 5% CO_2. During cell passage, the viability of the HaCaT cultures was determined to verify that a cytotoxic response was not occurring. Throughout the course of this experiment the viability at HaCaT splitting was found to be 95% or higher, indicating no loss of viability. This chronic dosing procedure continued for a total duration of 14 weeks (3 months) and was repeated with three independent sets to allow for the statistical analysis to be carried out. Silver nitrate exposed cells followed the same procedure for chronic delivery.

Silver nanoparticle retention. For quantitative analysis, HaCaT cells were seeded in a six-well plate at a density of 8×10^5 cells/well, dosed with their respective chronic Ag-NP concentrations, and incubated for 24 hours. The cells were then washed, detached with trypsin, counted, and digested with an aqueous solution of 0.05% Triton X-100, 3% HCl, and 1% HNO3. The amount of intracellular silver was then quantified through ICP-MS on a Perkin Elmer NexION 300D (Waltham, MA).

For cellular association studies, 2 x 10^5 cells were plated per chamber on a 2-well chambered slide and grown for 24 hours, keeping the same chronic treatment plan as previously outlined. The cells were then fixed with 4% paraformaldehyde and incubated with Alexa Fluor 555-phalloidin for actin staining and DAPI for nuclear staining (Invitrogen, Carlsbad, CA, USA). The slides were then sealed and imaged using a CytoViva 150 ultraresolution attachment on an Olympus BX41 microscope (Aetos Technologies, Inc., Auburn, AL, USA).

Confocal imaging and evaluation. In a 96-well plate HaCaT cells were seeded at a density of 2 x 10^5 per mL the day before experimentation. They were then dosed with the denoted Ag-NPs for 24 hours, followed by preparation for confocal imaging.[58] Briefly, cells were washed, fixed with 4% paraformaldehyde (Electron Microscopy Sciences), and permealized with 1% Triton-X100 (Sigma Aldrich). Fixed HaCaTs were then blocked with 1% bovine serum albumin (Sigma Aldrich), probed with the targeted primary and secondary antibodies, and imaged on a BD Pathway 435 confocal microscope using the DAPI, FITC and TRITC filters. Primary antibodies were used to evaluate p38 phosphorylation (Cell Signaling Technology), actin expression (Invitrogen), and ki67 quantities (Thermo Scientific); with the appropriate corresponding secondary antibodies (Thermo Scientific). Acquired images underwent analysis using the BD AttoVision™ and the BD Data Explorer software packages.

ELISA analysis. For determination of IL-6 and TNF-α the supernatants were removed daily and stored at -80 ºC until analysis. Concentrations of extracellular IL-6 and TNF-α were quantified using an ELISA kit (Invitrogen) in accordance with the manufacturer's protocol. The secreted concentrations of IL-6 and TNF- α were determined through the use of a set of standards following sequential dilution.

For Akt and Erk analyses, HaCaT cells were seeded in a 6-well plate at a density of 8 x 10^5 per well and incubated in serum free media containing the stated Ag-NP concentrations for 24 hours. Cells were then stimulated with 10 ng/mL EGF for 2 hours, after which they were lysed in a non-denaturing buffer (Cell Signaling Technology) containing phosphatase and protease inhibitors. The cell debris was removed *via* centrifugation at 15000 rpm for 15 minutes at 4 ºC. The supernatants were removed and stored at -80 ºC until analysis. The phosphorylation levels of Akt and Erk were ascertained with ELISA kits (Cell Signaling Technology) and normalized by the total amount of the same protein, quantified in parallel.

Real time PCR arrays. Cells were seeded in a 6-well plate at a density of 8×10^5 per well and incubated overnight. The following day HaCaT cultures were exposed to the stated Ag-NP conditions for a duration of 24 hours. For EGF dependent gene regulation, cells were incubated in serum free media then stimulated with 10 ng/mL EGF for 2 hours. The RNA was then isolated using the RNeasy Mini Kit (Qiagen), quantified on a NanoDrop spectrophotometer (Thermo Scientific), and processed for PCR array analysis with the RT2 First Strand kit (Qiagen). The PCR arrays (human stress and toxicity or human EGF/PDGF signaling - Qiagen) were run in accordance with the manufacturer's protocol.

Statistical analysis. Data is expressed as the mean ± the standard error of the mean (SEM). A two way ANOVA with a Bonferroni post-test was run using Graph Pad Prism to determine statistical significance. Significance was indicated for a p-value less than 0.05. PCR arrays were analyzed with the aid of the Qiagen software with denoted gene alterations have a fold regulation over 2.0 and p-value less than 0.05.

SUPPORTING INFORMATION AVAILABLE: Dose dependent Ag-NP toxicity, cytotoxicity following chronic exposure, stress response at concentrations of 0.4 and 4 pg/mL, EGF signaling efficiency at concentrations of 0.4 and 4 pg/mL, HaCaT response to acute exposure with a 5 μg/mL dose, and silver nitrate cytotoxicity. This information is available free of charge via the Internet at http://pubs.acs.org.

REFERENCES

1. Maynard, A. D. Nanotechnology: Assessing the Risks. *Nano Today* **2006**, *1*, 22–33.

2. Oberdörster, G.; Oberdörster, E.; Oberdörster, J. Nanotoxicology: An Emerging Discipline Evolving From Studies of Ultrafine Particles. *Environ. Health Perspect.* **2005**, *113*, 823–839.

3. Nel, A.; Xia, T.; Li, N. Toxic Potential of Materials at the Nanolevel. *Science* **2006**, *311*, 622–627.

4. Xia, T.; Li, N.; Nel, A. E. Potential Health Impact of Nanoparticles. *Annu. Rev. Public Health* **2009**, *30*, 137–150.

5. Hussain, S. M.; Braydich-Stolle, L. K.; Schrand, A. M.; Murdock, R. C.; Yu, K. O.; Mattie, D. M.; Schlager, J. J.; Terrones, M. Toxicity Evaluation for Safe Use of Nanomaterials: Recent Achievements and Technical Challenges. *Adv. Mater.* **2009**, *21*, 1549–1559.

6. Kang, G. S.; Gillespie, P. A.; Gunnison, A.; Moreira, A. L.; Tchou-Wong, K.; Chen, L. Long-Term Inhalation Exposure to Nickel Nanoparticles Exacerbated Atherosclerosis in a Susceptible Mouse Model. *Environ. Health Perspect.* **2011**, *119*, 176–181.

7. Stebounova, L. V.; Morgan, H.; Grassian, V. H.; Brenner, S. Health and Safety Implications of Occupational Exposure to Engineered Nanomaterials. *WIREs Nanomed. Nanobiotechnol.* **2012**, *4*, 310–321.

8. Arora, S.; Rajwade, J. M.; Paknikar, K. M. Nanotoxicology and *in Vitro* Studies: The Need of the Hour. *Toxicol. Appl. Pharmacol.* **2012**, *258*, 151–165.

9. Braydich-Stolle, L. K.; Speshock, J. L.; Castle, A. A.; Smith, M. M.; Murdoch, R. C.; Hussain, S. M. Nanosized Aluminum Altered Immune Function. *ACS Nano* **2010**, *4*, 3661–2670.

10. Elsaesser, A.; Howard, C. V. Toxicology of Nanoparticles. *Adv. Drug Delivery Rev.* **2012**, *64*, 129–137.

11. Sayes, C. M.; Reed; K. L.;Warheit, D. B. Assessing Toxicity of Fine and Nanoparticles: Comparing *in Vitro* Measurements to *in Vivo* Pulmonary Toxicity Profiles. *Toxicol. Sci.* **2007**, *97*, 163–180.

12. Warheit, D. B.; Sayes, C. M.; Reed, K. L. Nanoscale and Fine Zinc Oxide Particles: Can *in Vitro* Assays Accurately Forecast Lung Hazards Following Inhalation Exposures? *Environ. Sci. Technol.* **2009**, *43*, 7939–7945.

13. Wang, L.; Luanpitpong, S.; Castranova, V.; Tse, W.; Lu, Y.; Pongrakhananon, V.; Rojanasakul, Y. Carbon Nanotubes Induce Malignant Transformation and Tumorigenesis of Human Lung Epithelial Cells. *Nano Lett.* **2011**, *11*, 2796–2803.

14. Teeguarden, J. G.; Hinderliter, P. M.; Orr, G.; Thrall, B. D.; Pounds, J. G. Particokinetics *in Vitro*: Dosimetry Considerations for *in Vitro* Nanoparticle Toxicity Assessments. *Toxicol. Sci.* **2007**, *95*, 300–312.

15. National Institute of Occupational Safety and Health. Current Intelligence Bulletin 63: Occupational Exposure to Titanium Dioxide. DHHS (NIOSH) Publication Number 2011–160.

16. van Broekhuizen, P.; van Veelen, W.; Streekstra, W. H.; Schulte, P.; Reijnders, L. Exposure Limits for Nanoparticles: Report of an International Workshop on Nano Reference Values. *Ann. Occup. Hyg.* **2012**, *56*, 515–524.

17. AshaRani, P. V.; Mun, G. L. K.; Hande, M. P.; Valiyaveettil, S. Cytotoxicity and Genotoxicity of Silver Nanoparticles in Human Cells. *ACS Nano* **2009**, *3*, 279–290.

18. Braydich-Stolle, L. K.; Lucas, B.; Schrand, A.; Murdock, R. C.; Lee, T.; Schlager, J. J.; Hussain, S. M.; Hofmann, M. C. Silver Nanoparticles Disrupt GDNF/Fyn Kinase Signaling in Spermatogonial Stem Cells. *Toxicol. Sci.* **2010**, *116*, 577–589.

19. Carlson, C.; Hussain, S. M.; Schrand, A. M.; Braydich-Stolle, L. K.; Hess, K. L.; Jones, R. L.; Schlager, J. J. Unique Cellular Interaction of Silver Nanoparticles: Size-Dependent Generation of Reactive Oxygen Species. *J. Phys. Chem. B* **2008**, *112*, 13608–13619.

20. Comfort, K. K.; Maurer, E. I.; Braydich-Stolle, L. K.; Hussain, S. M. Interference of Silver, Gold, and Iron Oxide Nanoparticles on Epidermal Growth Factor Signal Transduction in Epithelial Cells. *ACS Nano* **2011**, *5*, 10000–100008.

21. Hussain, S. M.; Hess, K. L.; Gearhart, J. M.; Geiss, K. T.; Schlager, J. J. *In Vitro* Toxicity of Nanoparticles in BRL 3A Rat Liver Cells. *Toxicol. in Vitro* **2005**, *19*, 975–983.

22. Colvin, V. L. The Potential Environmental Impact of Engineered Nanomaterials. *Nat. Biotechnol.* **2003**, *21*, 1166–1170.

23. Yang, X.; Liu, J.; He, H.; Zhou, L.; Gong, C.; Wang, X.; Yang, L.; Yuan, J.; Huang, H.; He, L.; *et al*. SiO$_2$ Nanoparticles Induce Cytotoxicity and Protein Expression Alteration in HaCaT Cells. *Part. Fibre Toxicol.* **2010**, *7*, 1.

24. Liang, H.; Jin, C.; Tang, Y.; Wang, F.; Ma, C.; Yang, Y. Cytotoxicity of Silica Nanoparticles on HaCaT Cells. *J. Appl. Toxicol.* **2014**, *34*, 367–372.

25. DeBrosse, M. C.; Comfort, K. K.; Untener, E. A.; Comfort, D. A.; Hussain, S. M. High Aspect Ratio Gold Nanorods Displayed Augmented Cellular Internalization and Surface Chemistry Mediated Cytotoxicity. *Mater. Sci. Eng. C* **2013**, *33*, 4094–4100.

26. Comfort, K. K.; Maurer, E. I.; Hussain, S. M. The Biological Impact of Concurrent Exposure to Metallic Nanoparticles and a Static Magnetic Field. *Bioelectromagnetics*. **2013**, *34*, 500–511.

27. Elder, A.; Vidyasagar, S.; DeLouise, L. Physicochemical Factors that Affect Metal and Metal Oxide Nanoparticle Passage Across Epithelial Barriers. *WIREs Nanomed. Nanobiotechnol.* **2009**, *1*, 434–450.

28. Prabhu, S.; Poulose, E. K. Silver Nanoparticles: Mechanism of Antimicrobial Action, Synthesis, Medical Applications, and Toxicity Effects. *Int. Nano Lett.* **2012**, *2*, 32.

29. Drake, P. L.; Hazelwood, K. J. Exposure-related Health Effects of Silver and Silver Compounds: A Review. *Ann. Occup. Hyg.* **2005**, *49*, 575–585.

30. Nel, A .E.; Madler, L.; Velegol, D.; Xia, T.; Hoek, E. M. V.; Somasundaran, P.; Klaessig, F.; Castranova, V.; Thompson, M. Understanding Biophysicochemical Interactions at the Nano-Bio Interface. *Nat. Mater.* **2009**, *8*, 543–557.

31. Rivera Gil, P.; Oberdorster, G.; Elder, A.; Puntes, V.; Parak, W. J. Correlating Physico-Chemical with Toxicological Properties of Nanoparticles: The Present and the Future. *ACS Nano* **2010**, *4*, 5527–5531.

32. Lynch, I.; Salvati, A.; Dawson, K. A. Protein-Nanoparticle Interactions: What Does the Cell See? *Nat. Nanotechnol*. **2009***, 4*, 546–547.

33. Lundqvist, M.; Stigler, J.; Elia, G.; Lynch, I.; Cedervall, T.; Dawson, K. A. Nanoparticle Size and Surface Properties Determine the Protein Corona with Possible Implications for Biological Impacts. *Proc. Natl. Acad. Sci. U.S.A.* **2008**, *105*, 14265–14270.

34. Maurer, E. I.; Sharma, M.; Schlager, J. J.; Hussain, S. M. Systematic Analysis of Silver Nanoparticle Ionic Dissolution by Tangential Flow Filtration: Toxicological Implications. *Nanotoxicology* **2013**, 8, 718–727.

35. Kittler, S.; Greulich, C.; Diendorf, J.; Köller, M.; Epple, M. Toxicity of Silver Nanoparticles Increases During Storage Because of Slow Dissolution Under Release of Silver Ions. *Chem. Mater.* **2010***, 22*, 4548–4554.

36. Beer, C.; Foldbjerg, R.; Hayashi, Y.; Sutherland, D.S.; Autrup, H. Toxicity of Silver Nanoparticles – Nanoparticle or Silver Ion? *Toxicol. Lett.* **2012**, *208*, 286–292.

37. Untener, E. A.; Comfort, K. K.; Maurer, E. I.; Grabinski, C. M.; Comfort, D. A.; Hussain, S. M. Tannic Acid Coated Gold Nanorods Demonstrate a Distinctive Form of Endosomal Uptake and Unique Distribution within cells. *ACS Appl. Mater. Interfaces* **2013**, *11*, 8366–8373.

38. Yue, T.; Zhang, X. Cooperative Effect in Receptor-Mediated Endocytosis of Multiple Nanoparticles. *ACS Nano* **2012**, 6, 3196–3205.

39. Comfort, K. K.; Speltz, J. W.; Stacy, B. M.; Dosser, L. R.; Hussain, S. M. Physiological Fluid Specific Agglomeration Patterns Diminish Gold Nanorod Photothermal Characteristics. *Adv. Nanopart.* **2013**, *2*, 336–343.

40. Cho, W. S.; Duffin, R.; Howie, S. E.; Scotton, C. J.; Wallace, W. A.; MacNee, W.; Bradley, M.; Megson, I. L.; Donaldson, K. Progressive Severe Lung Injury by Zinc Oxide Nanoparticles; The Role of Zn^{2+} Dissolution Inside Lysosomes. *Part. Fibre Toxicol.* **2011**, *8*, 27.

41. Kim, J. A.; Aberg, C.; Salvati, A.; Dawson, K. A. Role of Cell Cycle on the Cellular Uptake and Dilution of Nanoparticles in a Cell Population. *Nat. Nanotechnol.* **2012**, *7*, 62–68.

42. Halliwell, B. Free Radicals, Proteins and DNA. Oxidative Damage Versus Redox Regulation. *Biochem. Soc. Trans.* **1996**, *24*, 521S.

43. Whitmarsh, A. J. A Central Role for p38 MAPK in the Early Transcriptional Response to Stress. *BMC Biol.* **2010**, *8*, 1–3.

44. Eom, H. J.; Choi, J. p38 MAPK Activation, DNA Damage, Cell Cycle Arrest and Apoptosis as Mechanisms of Toxicity of Silver Nanoparticles in Jurkat T Cells. *Environ. Sci. Technol.* **2010**, *44*, 8337–8342.

45. Ahamad, M.; Posgai, R.; Gorey, T. J.; Nielsen, M.; Hussain, S. M.; Rowe, J. J. Silver Nanoparticles Induced Heat Shock Protein 70, Oxidative Stress, and Apoptosis in *Drosophila Melanogaster*. *Tox. Appl. Pharm.* **2010**, *242*, 263–269.

46. Huot, J.; Houle, F.; Marceau, F.; Landry, J. Oxidative Stress–Induced Actin Reorganization Mediated by the p38 Mitogen-Activated Protein Kinase/Heat Shock Protein 27 Pathway in Vascular Endothelial Cells. *Circ. Res.* **1997**, *80*, 383–392.

47. Bullwinkel, J.*;* Baron-Lühr, B.; Lüdemann, A.; Wohlenberg, C.; Gerdes, J.; Scholzen, T. Ki-67 Protein is Associated with Ribosomal RNA Transcription in Quiescent and Proliferating Cells. *J. Cell. Physiol.* **2006**, *206*, 624–635.

48. Suliman, Y. A.; Ali, D.; Alarifi, S.; Harrath, A. H.; Mansour, L.; Alwasel, S. H. Evaluation of Cytotoxic, Oxidative Stress, Proinflammatory and Genotoxic Effect of Silver Nanoparticles in Human Lung Epithelial Cells. *Environ. Toxicol.* **2013**, doi: 10.1002/tox.21880.

49. Rangel-Frausto, M. S.; Pittet, D.; Costigan, M.; Hwang, T.; Davis, C. S.; Wenzel, R. P. The Natural History of the Systemic Inflammatory Response Syndrome (SIRS). *J. Am. Med. Assoc.* **1995**, *273*, 117–123.

50. Pastore, S.; Mascia, F.; Mariani, V.; Girolomoni, G. The Epidermal Growth Factor Receptor System in Skin Repair and Inflammation. *J. Invest. Dermotol.* **2008**, *128*, 1365–1374.

51. Egeblad, M.; Werb, Z. New Functions for the Matrix Metalloproteinsases in Cancer Progression. *Nat. Rev. Cancer* **2002**, *2*, 161–174.

52. Zhang, Y.; Wolf-Yadlin, A.; Ross, P. L.; Pappin, D. J.; Rush, J.; Lauffenburger, D. A.; White, F. M. Time-Resolved Mass Spectrometry of Tyrosine Phosphorylation Sites in the Epidermal Growth Factor Receptor Signaling Network Reveals Dynamic Modules. *Mol. Cell. Proteomics* **2005**, *4*, 1240–1250.

53. Kulthong, K.; Srisung, S.; Boonpavanitchakul, K.; Kangwansupamonkon, W.; Maniratanachote, R. Determination of Silver Nanoparticle Release from Antibacterial Fabrics Into Artificial Sweat. *Part. Fibre Toxicol.* **2010**, *7*, 8.

54. Qian, X.; Peng, X. H.; Ansari, D. O.; Yin-Goen, Q.; Chen, G. Z.; Shin, D. M.; Yang, L.; Young, A. N.; Wang, M. D.; Nie, S. *In Vivo* Tumor Targeting and Spectroscopic Detection with Surface-Enhanced Raman Nanoparticle Tags. *Nat. Biotechnol.* **2008**, *26*, 83–90.

55. Geiser, M.; Kreyling, W. G. Deposition and Biokinetics of Inhaled Nanoparticles. *Part. Fibre Toxicol.* **2010**, *7*, 2.

56. Murdock, R. C.; Braydich-Stolle, L.; Schrand, A. M.; Schlager, J. J.; Hussain, S. M. Characterization of Nanomaterial Dispersion in Solution Prior to *in Vitro* Exposure Using Dynamic Light Scattering. *Toxicol. Sci.* **2008**, *101*, 239–253.

57. Stopford, W.; Turner, J.; Cappellini, D.; Brock, T. Bioaccessibility Testing of Cobalt Compounds. *J. Environ. Monit.* **2003**, *5*, 675–680.

58. Braydich-Stolle, L. K.; Castle, A. B.; Maurer, E. I.; Hussain, S. M. Advantages of Using Imaged-Based Fluorescent Analysis for Nanomaterial Studies. *Nanosci. Meth.* **2012**, *1*, 137–151.

Graphical TOC Entry: